NASA TECHNICAL MEMORANDUM

NASA TM X-1070

NASA TM X-1070

INVESTIGATION OF A LIQUID-FLUORINE INDUCER AND MAIN-STAGE PUMP COMBINATION DESIGNED FOR A SUCTION SPECIFIC SPEED OF 20 000

by Walter M. Osborn

Lewis Research Center
Cleveland, Ohio

NATIONAL AERONAUTICS AND SPACE ADMINISTRATION • WASHINGTON, D. C. • MARCH 1965

NASA TM X-1070

INVESTIGATION OF A LIQUID-FLUORINE INDUCER AND MAIN-STAGE PUMP COMBINATION DESIGNED FOR A SUCTION SPECIFIC SPEED OF 20 000

By Walter M. Osborn

Lewis Research Center
Cleveland, Ohio

NATIONAL AERONAUTICS AND SPACE ADMINISTRATION

For sale by the Office of Technical Services, Department of Commerce,
Washington, D.C. 20230 -- Price $1.00

INVESTIGATION OF A LIQUID-FLUORINE INDUCER AND MAIN-STAGE PUMP COMBINATION DESIGNED FOR A SUCTION SPECIFIC SPEED OF 20 000

by Walter M. Osborn

Lewis Research Center

SUMMARY

18201

A low-pressure-rise, liquid-fluorine pump inducer was designed for operation at suction specific speeds of 20 000. The inducer was designed to operate in conjunction with a high-pressure main-stage impeller in order to improve the main-stage performance at low values of net positive suction head. The main-stage impeller was a modification of an impeller used in a previous investigation in that the three vanes at the pump inlet were removed back to the first row of splitter vanes in order to match the flow angles of the fluid leaving the inducer.

The inducer and main-stage combination was operated in liquid fluorine for a total of 16.7 minutes. For approximately 12 minutes, the combination was operating under cavitating-flow conditions with inducer suction specific speeds as high as 22 358. Inspection of the rotors revealed no indication of cavitation damage, and it is probable that cavitation damage will not be a problem in liquid-fluorine pumps for rocket applications.

At a net positive suction head of 29 feet (the lowest used), a maximum total-pressure rise of 547 pounds per square inch, a maximum flow rate of 225 gallons per minute, and a maximum overall efficiency of 0.62 were obtained. At a net positive suction head of 100.5 feet (the highest used), a maximum pressure rise of 547 pounds per square inch, a maximum flow rate of 302 gallons per minute, and a maximum efficiency of 0.635 were obtained. An increase of 41.5 percent in maximum flow rate was obtained for the performance of the pump with an inducer as compared with the performance of the pump without an inducer at approximately the same inlet total pressure.

Changing the seal configuration from back pressurizing with inert gas as in a previous investigation to venting the fluorine leakage from the seal as in the present investigation proved satisfactory. No fluorine reaction was observed with the titanium carbide and aluminum oxide materials used for the rotating shaft seals.

AUTHOR

INTRODUCTION

The potential gain in specific impulse and density impulse through the use of fluorine as the oxidant in hydrogen rocket engines has resulted in continuing research on pumps and other components suitable for operation in liquid fluorine. Operational problems caused by the extremely high reactivity and toxicity of liquid fluorine, however, have limited its use as a rocket propellant. Fortunately, it now appears that these problems may be resolved by the use of rigidly standardized handling procedures, careful selection of materials, meticulous cleaning procedures, and finally, by exposing the internal surfaces of the system to fluorine gas to form a passive or protective fluoride surface film before exposure to liquid fluorine.

An extensive research program is required to study the special problems involved in the operation of high-performance turborocket fluorine pumps that must operate in the cavitating-flow regime. The performance characteristics of a liquid-fluorine pump operating under conditions of cavitation must be evaluated. There may also be a cavitation-damage problem even though the pump only operates for short periods of time. It is possible that cavitation attack could remove the protective fluoride surface film from the rotor-blade surfaces and cause rapid blade erosion or allow the liquid fluorine to react violently with the exposed base metal. In addition, the design of the pump rotating shaft seal is critical. The seal materials must perform adequately and dissipate the frictional energy generated without reacting with the fluorine.

In order to investigate these problems, a series of liquid-fluorine-pump tests were initiated at the NASA Plum Brook Facility. The centrifugal pump used in the first of these investigations (ref. 1) was conservatively designed for essentially noncavitating operation at a suction specific speed of 7000. At this condition it produced a maximum pressure rise of 550 pounds per square inch and a maximum flow rate of 248 gallons per minute. Since the pump performed as anticipated at its design conditions, it was tested in the cavitating-flow regime. A maximum suction specific speed of approximately 12 000 was obtained in these tests. During 37 minutes of the total test time of 49 minutes, the pump operated in cavitating flow. Inspection of the pump rotor and the instrumentation indicated no cavitation damage.

In order to investigate further the effects of cavitation in liquid fluorine and to evaluate the operation of the rotating shaft seals, an inducer was designed to operate in combination with the centrifugal impeller of reference 1. The inducer and main-stage combination was designed to operate at a suction specific speed of 20 000 and still produce the design pressure and flow requirements of the main stage without an inducer.

This report presents the theoretical design for the inducer and the experimental results for the inducer - main-stage combination. The seal problems encountered during the investigation are discussed.

PUMP DESIGN CONSIDERATIONS

Main-Stage Impeller

The main-stage-pump impeller used in this investigation was a modification of the impeller used in the investigation of reference 1 in that the three vanes at the pump inlet were removed back to the first row of splitter vanes. This alteration was necessary to match the flow angles of the fluid leaving the inducer and entering the pump. The following parameters were used in the impeller design:

Pump speed, N, rpm	11 490
Pump outlet tip speed, U_3, ft/sec	198
Flow rate, Q, gal/min	248.5
Pressure rise across impeller, lb/sq in.	500
Suction specific speed, S	7000
Net positive suction head, H_{sv}, ft	76.5 (approx. 50 lb/sq in.)
Inlet hub-tip radius ratio, r_h/r_t	
(Before blade alteration)	0.40
(After blade alteration)	0.50
Efficiency	0.70
Impeller outlet diameter, in.	3.936
Impeller inlet tip diameter, in.	1.868
Slip factor	0.90
Number of blades at inlet (after blade alteration)	6
Blade shape	
From z = 0 to 0.858 in.	Parabolic
From z = 0.858 to 0.9984 in.	Straight
Blade elements	Radial
Blade thickness (perpendicular to mean camber line), in.	1/16

The impeller was designed by the stream filament method; the design procedure is discussed in reference 1.

Inducer Stage

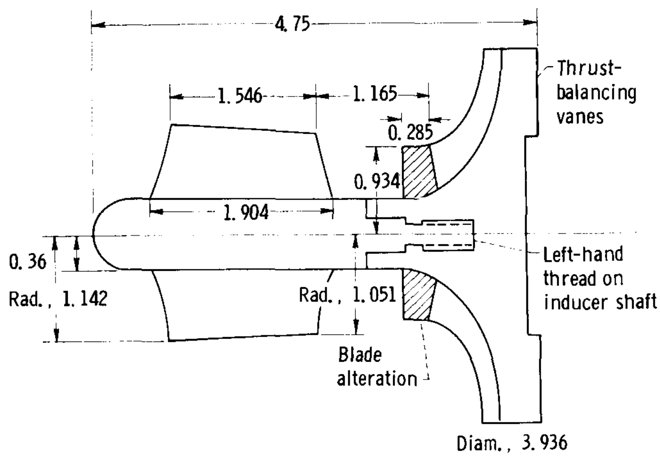

Figure 1. - Inducer and main-stage-pump profile in meridional plane. (All dimensions in inches.)

The inducer was designed to operate at a suction specific speed of 20 000 and to produce a head rise sufficient to enable the main stage to operate at its originally designed suction specific speed of 7000. This allowed a reduction in net positive suction head of 57.7 feet. Reference 2 was used for optimizing the inducer inlet tip radius for cavitating flow, and the optimized inlet tip angle was 80.6°. The inducer outer radius was tapered from a radius of 1.142 inches at the inlet to a radius of 1.051 inches at the outlet. The inducer hub radius was chosen the same as the hub radius of the main stage (0.36 in.) and was constant through the inducer. Figure 1 shows the inducer and main-stage profiles in the meridional plane and gives the major dimensions used in the inducer design. Also shown is the blade alteration to the main stage. The inducer and the modified main stage were separated by approximately 1.165 inches at the shroud. A photograph of the combination is shown in figure 2 (taken before the fluorine run). The following parameters were used in the inducer design:

Solidity	2.025
Number of blades	3
Blade thickness (perpendicular to mean camber line), in.	1/16
Suction specific speed, S	20 000
Net positive suction head, H_{sv}, ft	18.8
Head rise across inducer, ΔH, ft	57.7
Flow rate, Q, gal/min	248.5
Inducer speed, N, rpm	11 490
Inlet tip diameter, in.	2.284

In the design of the inducer, the total flow is divided into 10 equal increments at inlet and outlet. The assumption of uniform axial velocity at the inducer inlet locates the inlet streamlines and determines the inlet velocity diagrams. The location of the outlet

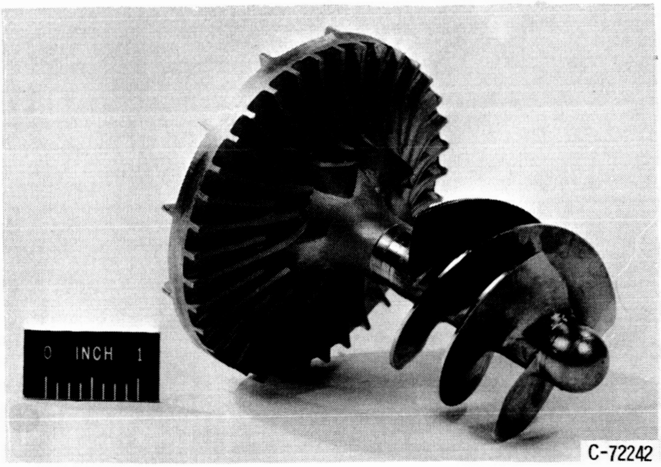

Figure 2. - Liquid-fluorine inducer and main-stage pump.

streamlines and the outlet conditions may be determined by assuming an axial velocity $V_{z,2}$ at the shroud streamline and iterating a form of the radial equilibrium equation to satisfy continuity. The equation may be developed as follows.

For simple radial equilibrium

$$\frac{\Delta h_2}{\Delta r} = \frac{V_{\theta,2}^2}{rg} \tag{1}$$

(All symbols are defined in appendix A.) If the subscripts k and j denote adjacent radial stations and the trapezoidal rule is used for summation, equation (1) may be written

$$h_{2,k} - h_{2,j} = \frac{1}{2}\left(\frac{V_{\theta,2,k}^2}{r_{2,k}} + \frac{V_{\theta,2,j}^2}{r_{2,j}}\right)\frac{r_{2,k} - r_{2,j}}{g} \tag{2}$$

From Bernoulli's equation and vector diagrams

$$h_{2,k} - h_{2,j} = H_{1,k} - H_{1,j} + \Delta H_k - \Delta H_j - \frac{V_{z,2,k}^2}{2g} + \frac{V_{z,2,j}^2}{2g} - \frac{V_{\theta,2,k}^2}{2g} + \frac{V_{\theta,2,j}^2}{2g} \tag{3}$$

Substituting equation (3) into equation (2) and assuming a constant head at the inlet $(H_{1,k} = H_{1,j})$ give the equation as used in the inducer design

$$V_{z,2,j}^2 = V_{z,2,k}^2 + 2g(\Delta H_j - \Delta H_k) - (V_{\theta,2,j}^2 - V_{\theta,2,k}^2) - \left(\frac{V_{\theta,2,j}^2}{r_{2,j}} + \frac{V_{\theta,2,k}^2}{r_{2,k}}\right)(r_{2,j} - r_{2,k}) \tag{4}$$

The value $V_{\theta,2}$ may be obtained from

$$\Delta H_{ideal} = \Delta H + \Delta H_{loss} \tag{5}$$

where

$$\Delta H_{ideal} = \frac{U_2 V_{\theta,2} - U_1 V_{\theta,1}}{g}$$

$$\Delta H_{loss} = \frac{\bar{\omega} V_1'^2}{2g}$$

Thus

$$V_{\theta,2} = \frac{g\,\Delta H + \dfrac{\bar{\omega} V_1'^2}{2} + U_1 V_{\theta,1}}{U_2} \tag{6}$$

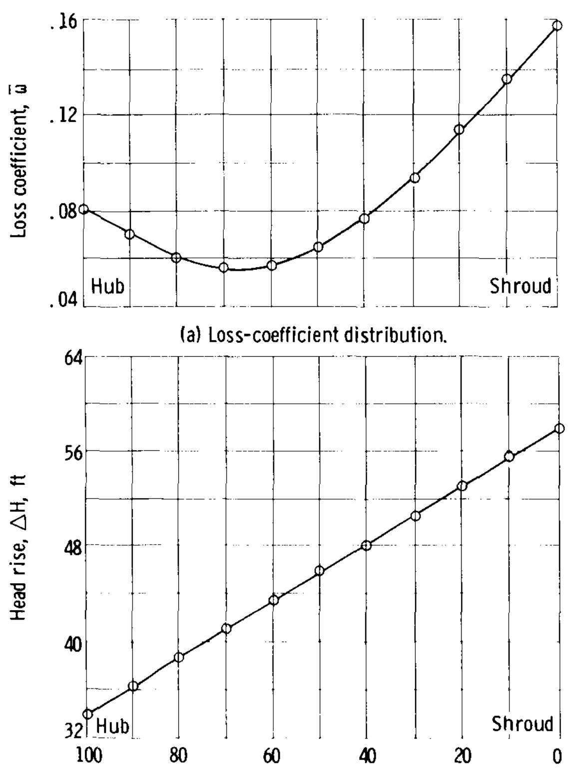

(a) Loss-coefficient distribution.

(b) Head-rise distribution.

Figure 3. - Inducer design parameters.

where $U_1 V_{\theta,1} = 0$ with no prewhirl at the inlet. The design procedure consists in assigning a value for $V_{z,2,k}$ at the shroud streamline and locating the adjacent streamline. The process is continued until all the streamlines are located and $\sum \Delta Q = Q$. If the radius of the hub streamline is not the same as the predetermined hub-streamline radius, a new value of $V_{z,2,k}$ at the shroud streamline is chosen and the procedure is repeated. After a distribution of $V_{z,2}$ is found that satisfies the chosen hub radius, the outlet vector diagrams may be completed. The distribution of the loss coefficient $\bar{\omega}$ used in the design is given in figure 3(a) and is based on the results of inducer tests conducted in the Lewis water tunnel. The distribution of the total head rise ΔH is assumed and is given in figure 3(b).

The blade is defined by circular arc sections on conical surfaces through the design streamline radii. These sections are stacked

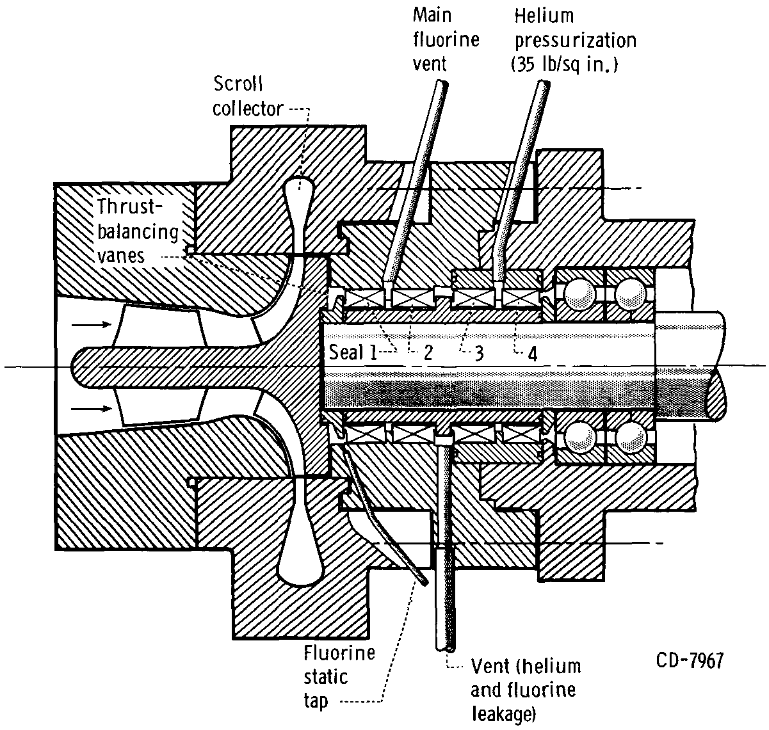

Figure 4. - Liquid-fluorine pump assembly.

to form a cambered blade. The blade coordinates are not given because of the large number of points required to define the blade.

APPARATUS AND METHODS

Pump Assembly

A 2.284-inch-diameter inducer was fabricated in Monel from the design information described in the preceding section. The inducer was attached to the modified main stage with a threaded shaft, as shown in figure 1. A sketch of the pump assembly is shown in figure 4. The assembly was similar to that used in reference 1 except for a change in the seal configuration and the stationary shroud surrounding the inducer and the main stage. The radial clearance between the rotating parts and the stationary shroud was approximately 0.030 inch. The seal configuration was altered to vent fluorine leakage from the primary liquid-fluorine seal (seal 1, fig. 4) instead of back pressurizing with helium gas as in the previous investigation (discussed in appendix B).

Test Facility

The liquid-fluorine pump facility is shown schematically in figure 5. The facility is a closed-loop system in which the liquid fluorine is circulated by the research pump.

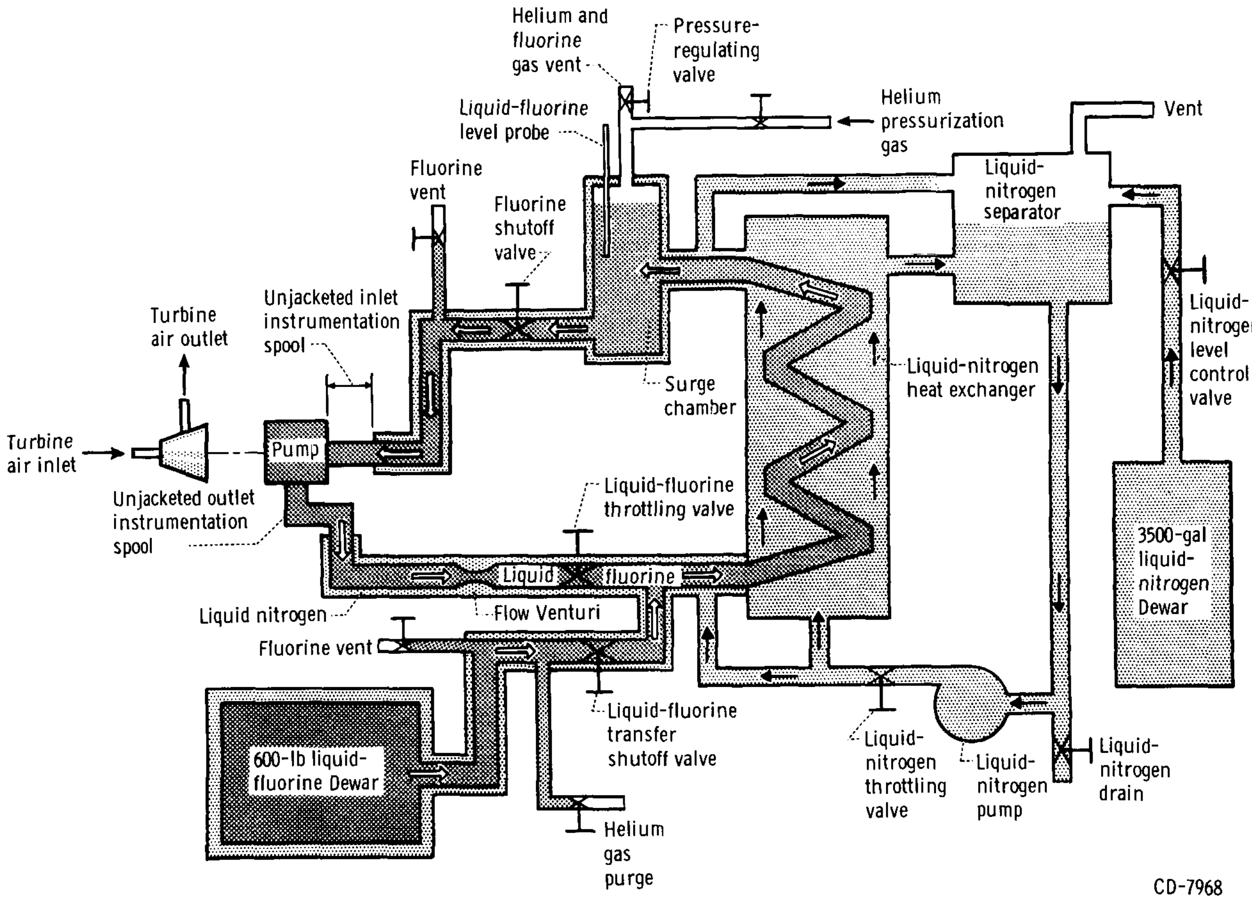

Figure 5. - Schematic of liquid-fluorine pump facility.

Liquid nitrogen is used as a coolant in a heat exchanger and in jackets and troughs surrounding the liquid-fluorine lines in order to obtain long test times. The pump and the inlet and outlet instrumentation spools were not covered with a liquid-nitrogen jacket. The test facility was a modification of that described in reference 1 in that the research pump and the drive turbine were placed outside the building in a concrete revetment (open on the top and at the front). Also, the containment vault was removed from around the pump because experience indicated that it was of little value, as burnouts generally occurred in the area of the rotating shaft seal or the seal vent. Thus, the research pump became readily accessible for mechanical installation and teardown. All fluorine vent lines vented waste fluorine gas directly to the atmosphere without creating an undue hazard. Only those areas directly downwind were controlled. Operation of the test loop is described in reference 1.

Instrumentation

The inlet instrumentation was located approximately 7 inches upstream of the inducer inlet in an unjacketed instrumentation spool piece (fig. 5). The inlet instrumentation consisted of two total-pressure probes, two manifolded static-pressure taps, and an encased platinum resistor probe for temperature measurement. The outlet instrumentation was located approximately 2 inches downstream of the outlet of the scroll collector and was similar to the inlet instrumentation. Static-pressure taps were also located 1/4 inch upstream and downstream of the inducer. Temperature and pressure measurements were taken in the Venturi section for flow-rate measurement. A magnetic speed pickup was used for speed measurement, and a strain-gage-type torquemeter located between the pump and the turbine was used to determine the power input to the pump.

All pressure measurements were taken with calibrated pressure transducers. The temperature probes were calibrated at two points by dipping the probes in liquid nitrogen and liquid oxygen. The torquemeter was calibrated statically by using a torque arm and deadweights. All instrumentation was calibrated electronically before and after the run.

All research data were recorded on magnetic tape in conjunction with a high-speed digital recorder.

PUMP PERFORMANCE

The data presented in this investigation were obtained in three pump runs for a total operating time of 16.7 minutes in liquid fluorine. The pressure rise as a function of flow rate was obtained in the first run (4.2 min) at four net positive suction heads corresponding to the inlet total pressures of reference 1 so that the performance of the main stage with and without an inducer could be compared. The flow rate was higher than anticipated at the high net positive suction heads, however, so that a second run (6.5 min) using a higher range pressure transducer for flow measurements was required to complete the curves. In the third run (6.0 min) the cavitation performance of the pump was evaluated by lowering the net positive suction head from a high value until the pressure rise deteriorated, while the speed and the flow rate were held constant. The three runs were conducted approximately 1 week apart.

The performance of the pump with the inducer at a design speed of 11 490 rpm is shown in figure 6. Figure 6(a) shows the performance curves for the total-pressure rise across the pump as obtained from total-pressure probes at the inlet and the outlet of the pump. The curves represent overall conditions measured downstream of the scroll collector. The solid symbols indicate the data that were obtained in the second run by using a higher range pressure transducer for flow measurement than was used in the first run. The slight discontinuity between the data of the two runs is within the accuracy range of the instrumentation. At flow rates less than 205 gallons per minute, the pump performance was approximately the same at all net positive suction heads, and an average

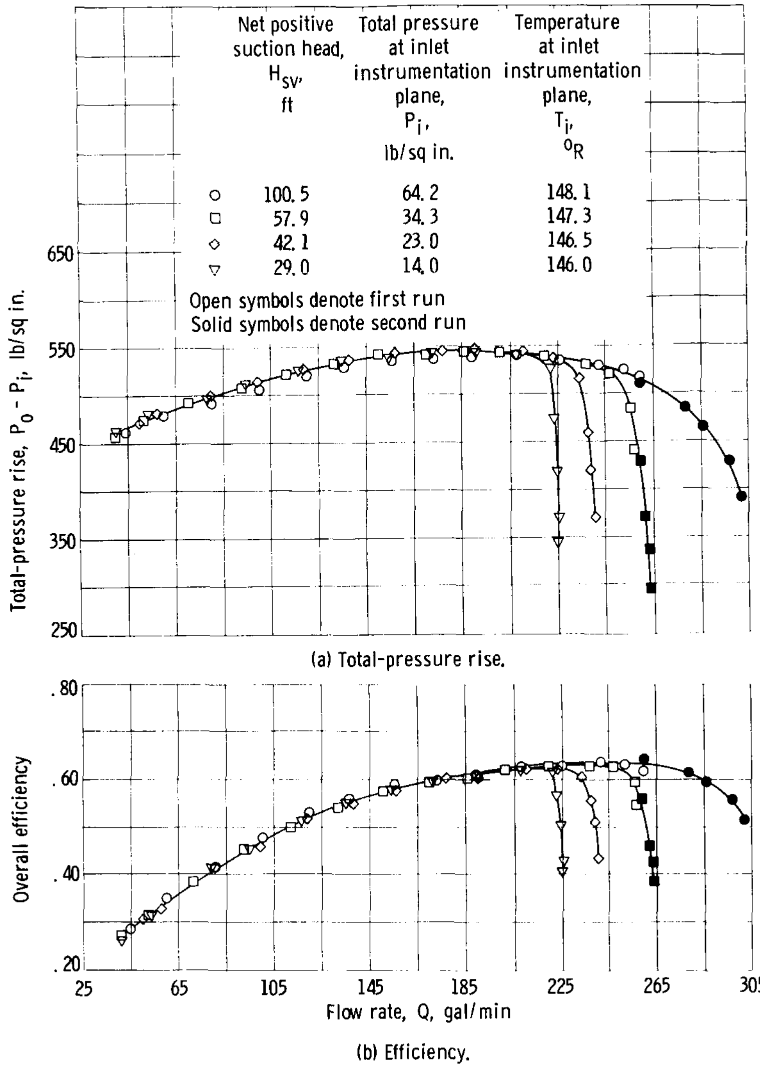

Figure 6. - Liquid-fluorine pump performance at several net positive suction heads. Pump speed, 11 490 rpm.

curve is shown through the data points. A maximum total-pressure rise of approximately 547 pounds per square inch was obtained at a flow rate of 185 gallons per minute for net positive suction heads between 29.0 and 100.5 feet. The maximum flow rate decreased from 302 to 225 gallons per minute as the net positive suction head was decreased from 100.5 to 29.0 feet. This dropoff in maximum flow rate as the net positive suction head was lowered indicates the loss in pump performance due to cavitation. Figure 6(b) presents the overall efficiency based on the pump total-pressure rise for various flow rates. At flow rates less than 205 gallons per minute, the efficiency is approximately the same for all net positive suction heads used in the tests, and an average curve is drawn through the data points. The curve for a net positive suction head of 100.5 feet represents essentially noncavitating performance, and a maximum ef-

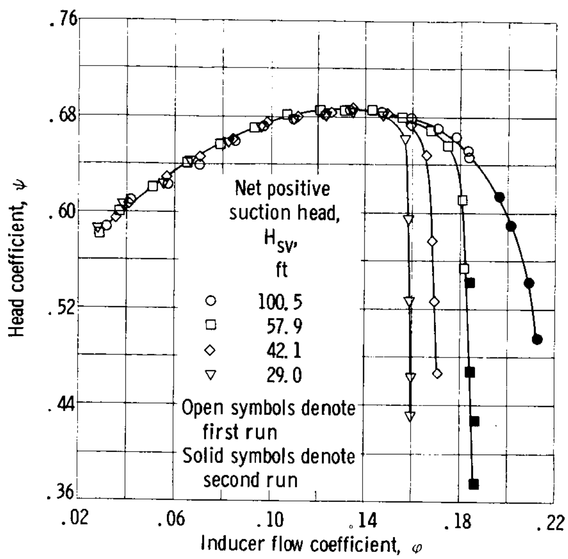

Figure 7. - Overall performance of liquid-fluorine pump at several net positive suction heads.

ficiency of approximately 0.635 was obtained. At the lowest net positive suction head (29.0 ft), the maximum efficiency was approximately 0.62 as cavitation limited the flow range and prevented the maximum-efficiency point (noncavitating) from being reached.

Figure 7 presents the performance of the pump with the inducer in terms of head coefficient and flow coefficient for four net positive suction heads. The maximum head coefficient was 0.685. The head coefficients for the pump with an inducer (0.685) and without an inducer (0.688, ref. 1) were approximately the same, which indicates that the blade alteration of the main stage used in this investigation did not adversely affect the main-stage pump performance.

The inducer static-pressure rise as determined by wall static-pressure taps located

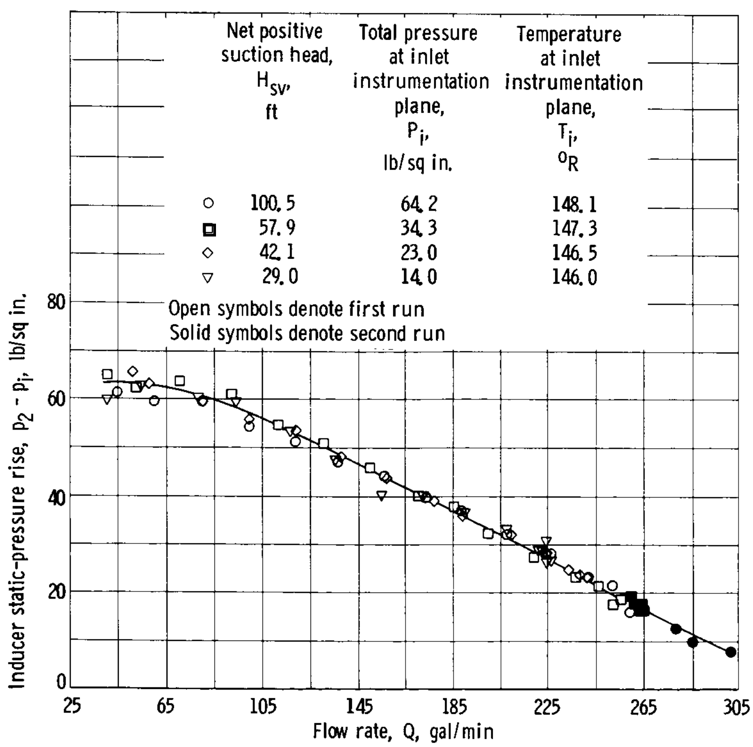

Figure 8. - Inducer static-pressure rise. Inducer speed, 11 490.

approximately 7 inches upstream of the inducer and 1/4 inch downstream of the inducer is shown as a function of flow rate in figure 8. An average curve has been drawn through the data points for the various net positive suction heads, and the pressure-rise - flow-rate relation is approximately a straight line. The slight falloff in the slope of the curve at the low flow rates (high pressure rise) is probably caused by secondary flows (recirculation) at the inducer inlet tip and leakage due to the relatively large radial clearance (0.030 in.) between the inducer and the stationary shroud. Since approximately the same performance is obtained at all net positive suction heads tested, it appears that cavitation is not of sufficient magnitude to affect the performance of the inducer. Performance of the inducer at low values of net positive suction head (29.0 and 42.1 ft) was not obtained at flow rates higher than 225 gallons per minute because cavitation in the main stage limited the flow rate. The inducer produced its design pressure rise of 38 pounds per square inch at a flow rate of 181 gallons per minute. This is considerably below the inducer design flow rate of 248 gallons per minute and is due to idealized design calculations that assume zero-thickness blades. Thus, the performance of the inducer - main-stage combination could probably be improved at lower values of net positive suction head with a better matching of the inducer and the main stage.

The cavitation performance of the liquid-fluorine pump is presented in figure 9(a). In these tests, the flow rate and the speed were held constant and the net positive suction head was lowered until the pump pressure rise deteriorated. At the high flow rates, the pump pressure rise began gradually to fall off at high values of net positive suction head. At the lower flow rates, the pump pressure rise remained constant over a large range of net positive suction heads but deteriorated very rapidly at low values of net positive suction head. These curves are similar to cavitation performance curves for other fluids and

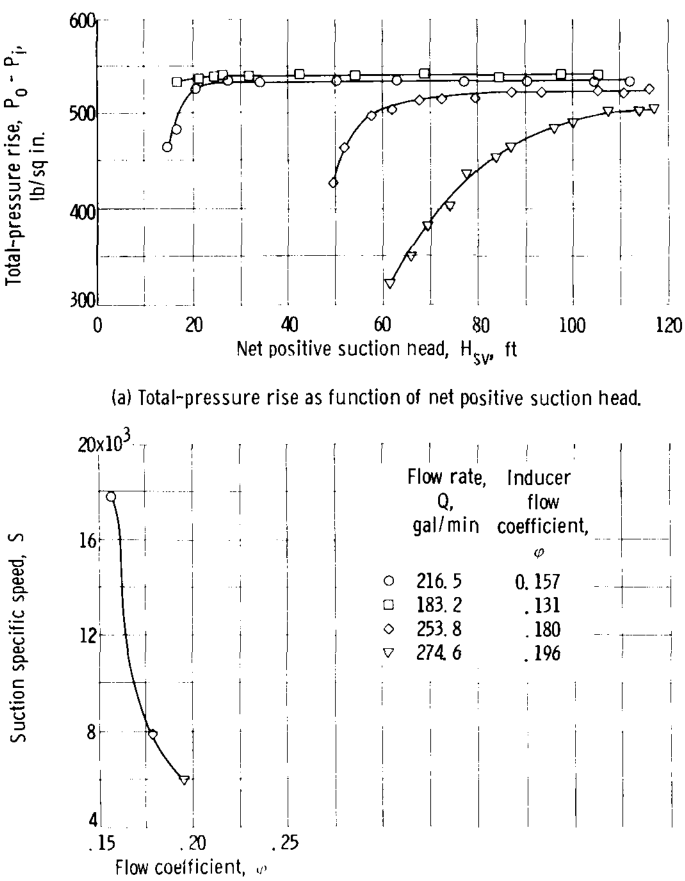

(a) Total-pressure rise as function of net positive suction head.

(b) Inducer suction specific speed at 2-percent dropoff in pressure rise.

Figure 9. - Cavitation performance of liquid-fluorine pump at four flow rates Pump speed, 11 490 rpm.

indicate that the mechanism of cavitation in liquid fluorine is similar to that in other fluids. At the last point on the curve for a flow coefficient of 0.157 (pressure rise = 465 lb/sq in., H_{sv} = 15 ft), the inducer was operating at a suction specific speed of 22 358. This is the maximum suction specific speed at which the inducer was tested. Figure 9(b) is a plot of flow coefficient as a function of the suction specific speed at which the inducer was operating when a 2-percent loss in pressure rise occurred as the net positive suction head was lowered. The values were obtained from figure 9(a). At a high value of flow coefficient (0.196), a 2-percent decrease in pressure rise occurred at a relatively low value of inducer suction specific speed (6000) because of the cavitation in the main stage. As the flow coefficient was decreased to 0.157, the inducer suction specific speed increased to 17 800 before the dropoff occurred. Only a 1-percent dropoff in pressure rise was obtained for a flow coefficient of 0.131, since the net positive suction head was not reduced to a low enough value during the tests. At this point, the inducer was operating at a suction specific speed of 18 390. An extrapolated value of suction specific speed for a 2-percent dropoff in pressure rise at a flow coefficient of 0.131 would be approximately 20 400.

During the tests in this investigation, the inducer - main-stage combination was operated in liquid fluorine with cavitating-flow conditions for approximately 12 minutes with suction specific speeds as high as 22 358. Visual inspection of the inducer and main stage revealed no indication of cavitation damage. Thus, it is probable that cavitation damage will not be a problem in liquid-fluorine pumps for rocket applications.

Figure 10 presents a comparison of the performance of the pump with and without

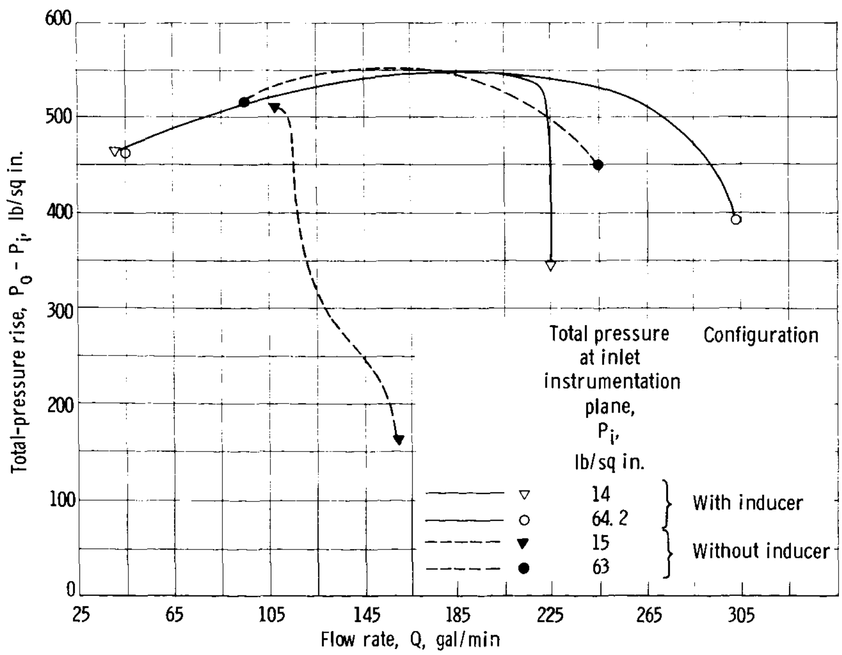

Figure 10. - Performance comparison of pump with and without inducer at two inlet total pressures.

an inducer. The tests were run at approximately the same inlet pressures (same net positive suction heads). The main stage used in this investigation, however, has been altered to match fluid flow angles coming out of the inducer. The gain in performance may be seen by comparing the dashed curves of figure 10 with the solid curves for the corresponding inlet total pressures. As expected, the greatest performance gains were at the lower inlet pressure (~14 lb/sq in.) where the addition of the inducer increased the maximum flow rate 41.5 percent.

SUMMARY OF RESULTS

Data for a liquid-fluorine inducer and main-stage pump combination designed for a suction specific speed of 20 000 were obtained in three runs with a total operating time of 16.7 minutes in liquid fluorine. The following results were realized from the investigation:

1. At a net positive suction head of 100.5 feet, a maximum pressure rise of 547 pounds per square inch, a maximum flow rate of 302 gallons per minute, and a maximum efficiency of 0.635 were obtained.

2. At a net positive suction head of 29 feet, a maximum pressure rise of 547 pounds per square inch, a maximum flow rate of 225 gallons per minute, and a maximum efficiency of 0.62 were obtained.

3. An increase of 41.5 percent in maximum flow rate was obtained for the performance of the pump with an inducer as compared with the performance of the pump without an inducer at approximately the same inlet total pressure (~14 lb/sq in.).

4. It is probable that cavitation damage will not be a problem in liquid-fluorine pumps for rocket applications. Inspection of the rotors used in this investigation revealed no damage from approximately 12 minutes of operation under cavitating-flow conditions with suction specific speeds as high as 22 358.

5. The titanium carbide and aluminum oxide materials used for the rotating shaft seals in this investigation showed no reaction with liquid fluorine and adequately performed their functions as seal materials.

Lewis Research Center,
National Aeronautics and Space Administration,
Cleveland, Ohio, December 2, 1964.

APPENDIX A

SYMBOLS

g acceleration due to gravity, ft/sec^2

H total head, ft

ΔH total head rise, ft

H_{SV} net positive suction head, $H_i - h_v$, ft

h static head, ft

Δh static head rise, ft

h_v vapor head, ft

N pump speed, rpm

P total pressure, lb/sq in.

p static pressure, lb/sq in.

Q flow rate, gal/min

r radius measured from axis of rotation, ft

S suction specific speed, $N\sqrt{Q}/H_{SV}^{3/4}$

T temperature, $^{\circ}R$

U tip speed, ft/sec

V velocity, ft/sec

V' relative velocity, ft/sec

z axial distance, in.

φ inducer flow coefficient, $V_{z,1}/U_1$

ψ head coefficient, $g\,\Delta H/U_3^2$

$\bar{\omega}$ loss coefficient, $\Delta H_{loss}\Big/V_1'^2/2g$

Subscripts:

h hub

i inlet instrumentation plane (approximately 7 in. upstream of inducer)

j,k adjacent radial stations

o outlet instrumentation plane (downstream of scroll collector)

t inlet blade tip

z axial direction

θ tangential plane

1 inducer inlet

2 inducer outlet

3 main stage outlet

APPENDIX B

DISCUSSION OF SEAL PROBLEMS

In the test of the main stage without an inducer (ref. 1), the primary liquid-fluorine seal was a bellows seal with a graphitic-carbon nosepiece that rubbed against a rotating Nitralloy mating ring. The primary seal was backed up by a similar secondary seal. The cavity between the two seals was pressurized with helium gas to a slightly higher pressure than the pressure of the liquid fluorine behind the pump rotor. Helium leakage was vented after the secondary seal. Thus, the seals operated with a sweep gas across the rubbing surfaces. Such an arrangement proved successful, and the pump of reference 1 was operated for 49 minutes in liquid fluorine with the same seals.

A test of a commercial pump with the same seal materials but with the fluorine leakage vented from the primary seal resulted in a burnout in the seal-vent area, which caused extensive damage to the pump and the test equipment.

Early tests with the inducer and the pump of this investigation and the same materials and seal arrangements as in reference 1 resulted in two aborts at startup with burning in the seal-vent area. This was due to large oscillations in the inlet pressure caused by a defective controller that caused the primary seal to unseat and let fluorine into the seal-vent area. Damage in both cases was minor since the primary fluorine seal and the helium backup gas contained the liquid fluorine in the test loop. In both cases the graphitic-carbon nosepiece of the secondary seal was consumed.

The commercial pump was tested again with a redesigned seal configuration similar to that used in the investigation of reference 1 (helium seal dam) and similar seal materials (graphitic nosepiece). These tests resulted in two good runs. On the third run, a detonation occurred, but no burning followed. All parts were recovered except a graphitic-carbon wear ring (the same material as used in the primary seal) surrounding the shrouded inducer and the primary-bellows-seal graphitic-carbon nosepiece. The detonation was attributed to a reaction between fluorine and the graphitic-carbon wear ring. Static tests of samples of the graphitic material soaked in liquid fluorine also produced a reaction, if the soak time was long enough. It is believed that graphitic material that has had adequate soak time in liquid fluorine will enable an unstable carbon monofluoride to be formed interstitially in the graphitic material, which may react violently.

At this point, an investigation for new seal materials suitable for rotating shaft seals for liquid-fluorine pumps was initiated. The seal tests (ref. 3) indicated that flame-plated aluminum oxide and titanium carbide cermet (nickel binder) are potential seal materials and that the presence of a fluoride film formed during sliding (nickel fluoride) is beneficial in reducing friction and wear of materials in liquid fluorine.

Based on the results of reference 3, the seal materials for seals 1, 2, and 3 (fig. 4, p. 7) were changed to a titanium carbide (nickel binder) for the rotating mating ring and to a flame-plated aluminum oxide for the nosepiece of the bellows seal. Graphite and Nitralloy were retained for seal 4 (oil seal). The seal configuration was also changed to vent fluorine leakage from the primary seal (seal 1), and a low-range pressure transducer was placed in the vent line as a warning device to signal a possible seal failure.

The tests of this investigation were planned for relatively short running times (4 to 6 min) in order to inspect the seals to determine seal wear rates. None of the tests were terminated by seal failure or excessive fluorine leakage. Inspection of the materials after the runs indicated that the materials were able to dissipate the frictional energy generated without reacting with the fluorine. The wear rate of the flame-plated aluminum oxide nosepiece (originally 0.008 to 0.010 in. thick) was higher than might be anticipated from the results of reference 3. The bellows seal used for the tests of reference 3, however, was of a different construction and used a different grade of flame-plated aluminum oxide as compared with the shaft seals used in this investigation. Also, the test conditions for the investigation of reference 3 were different from the operating conditions for the pump seal in that the total seal-face load (15 lb) and sliding velocity (2300 ft/min) were approximately one-third that of the operating conditions for the pump seals. As the greatest wear occurred in the primary fluorine seal (seal 1), it is the only one discussed here. For the three runs lasting 4.2, 6.5, and 6.0 minutes, the maximum total seal loads (spring load plus pressure balance face load) were 53, 48 and 38 pounds, respectively. This reduction in total seal load was accomplished by reducing the spring load of the bellows seal, since the maximum pressure balance load was approximately 30 pounds for all runs. After the 4.2-minute run, there was approximately 0.003 inch of aluminum oxide remaining (0.008 to 0.010 in. originally) on 80 percent of the circumference of the nosepiece, and 20 percent of the circumference was exposed base metal where the aluminum oxide appeared to have flaked off. There was no appreciable wear on the titanium carbide mating ring. Inspection of seal 1 after the 6.5-minute run showed 75 percent of the circumference of the aluminum oxide nosepiece worn down to the base metal, and the remaining aluminum oxide was very thin. Metal-to-metal contact occurred between the mating ring and the end plate of the bellows seal, but the mating ring was only slightly grooved. After the 6-minute test (lowest seal loading) there was approximately 0.005 inch of aluminum oxide remaining on the nosepiece. Some of the aluminum oxide, however, chipped out on disassembly, which indicated a poor bond between the aluminum oxide and the base metal. The mating ring was slightly rough but was not grooved.

A separate investigation was made of a bellows-type rotating shaft seal similar to the ones used in this report. The seal was instrumented with accelerometers and tested in liquid nitrogen, and the test results indicated that considerable seal chatter occurred during the tests. If seal chattering were present during the fluorine tests, it could be a contributing cause of the high wear rates and the flaking off of the aluminum oxide noisepiece. Thus, the relatively high wear rates experienced on the aluminum oxide nosepieces used in this investigation as compared with the results of reference 3 were believed due to seal chattering, higher sliding velocities, higher seal-face loads, a different grade of aluminum oxide, and a poor bond between the flame-plated aluminum oxide and the metallic base.

Since the completion of the tests of this investigation, several hours of running time have been accumulated with both research and commercial pumps incorporating the new seal materials. There has been no evidence of a reaction of the seal materials with the liquid fluorine, and the seal wear rates have been acceptable for fluorine pumps for rocket applications.

REFERENCES

1. Osborn, Walter M.: Noncavitating and Cavitating Performance of a Liquid-Fluorine Pump Designed by Stream-Filament Method. NASA TM X-722, 1963.

2. Ross, C. C., and Banerian, Gordon: Some Aspects of High-Suction Specific-Speed Pump Inducer. Trans. ASME, vol. 78, no. 3, Nov. 1956, pp. 1715-1721.

3. Hady, W. F., Allen, G. P., Sliney, H. E., and Johnson, R. L.: Friction, Wear, and Dynamic Seal Studies in Liquid Fluorine and Liquid Oxygen. NASA TN D-2453, 1964.